OPTIMIZED SILICON SOLAR CELLS

FOR

SPACE EXPLORATION POWER SYSTEMS

TECHNICAL REPORT

Peter A. Iles
James M. Palmer

August 7, 1970

JPL Contract No. 952865

Centralab Semiconductor
Globe-Union Inc.
4501 N. Arden Drive
El Monte, California 91734

OPTIMIZED SILICON SOLAR CELLS

FOR

SPACE EXPLORATION POWER SYSTEMS

TECHNICAL REPORT

Peter A. Iles
James M. Palmer

August 7, 1970

JPL Contract No. 952865

Centralab Semiconductor
Globe-Union Inc.
4501 N. Arden Drive
El Monte, California 91734

This work was performed for the Jet Propulsion Laboratory, California Institute of Technology, as sponsored by the National Aeronautics and Space Administration under the Contract NAS 7-100.

This report contains information prepared by Centralab Semiconductor, a Division of Globe-Union Inc., under JPL Subcontract No. 952865.

Its content is not necessarily endorsed by the Jet Propulsion Laboratory, California Institute of Technology or the National Aeronautics and Space Administration.

ABSTRACT

This report describes in detail several studies relating to the improvement of silicon solar cells and their optimization for operation in the vicinity of Mercury and Venus. The studies have been conducted in the areas of thermal characteristics and series resistance. As a result of these studies near-optimum cells have been designed for Mercury and Venus missions. Experimental cell fabrication will resolve the remaining factors.

TABLE OF CONTENTS

LIST OF FIGURES

1.0 Summary

This is the first of a two-part analysis report describing results obtained during a study of silicon solar cells optimized for space exploration power systems. This part describes the development of silicon solar cells for operation at Mercury and Venus. A subsequent report will describe solar cells for Mars, Asteroid Belt and Jupiter operation.

The objective of the program is to devlop optimized silicon solar cells for use on spacecraft missions operable at heliocentric orbits between 0.1 and 15 AU. The investigation is both theoretical and experimental in nature.

For these near-sun missions, the major loss factor is internal series resistance, and means to reduce this resistance have been studied. The important variables were diffusion sheet resistance, bulk resistivity and contact pattern. In addition, cells for Mercury operation have been designed to reflect a significant portion of the incident radiation to decrease the cell temperature.

An equation was developed to relate output power to incident irradiation and cell temperature over a reasonably wide range of operation. This equation was used in the reflecting area optimization but can be used for design purposes as well.

A hypothesis that shifting the anti-reflection coating wavelength would provide more power from a Mercury cell was tested and proven false.

Some of the theoretical conclusions are rather broad and precise values cannot be justified. Experimental cell fabrication is necessary to determine these values. The next phase of the program will include experimental cell fabrication to optimize these factors. Upon optimization, an attempt will be made to express them theoretically for future analysis.

2.0 Introduction

This is the first part of a two-part analysis report detailing results obtained during study of solar cells for space exploration power systems. This part details the development of solar cells for Mercury and Venus flights. For these near-sun missions, the major loss factor is internal series resistance, and means to reduce this loss have been studied. Variables included base resistivity, diffused layer sheet resistance and contact pattern. An equation giving power as a function of solar irradiance and cell temperature was derived and applied to a computer program to find the optimum reflecting area for Mercury cells. The effects of shifting the anti-reflection coating thickness was studied. A complete synopsis of all design variables is included.

3.0 Technical Discussion

3.1 Equilibrium Temperature:

The equilibrium temperature of a solar cell in free space (i.e. incident radiation from the sun alone) is dependent upon several factors, most notably the optical characteristics of the surfaces and the amount of incident radiation. The equation

$$T = \left[\frac{\alpha_S}{\epsilon_F + \epsilon_B} * \frac{S \cos \theta \ (1-\eta)}{D^2 \ \sigma}\right]^{0.25} \qquad (1)$$

where

T = equilibrium temperature (K)

α_S = front surface solar absorptance

ϵ_F = front surface thermal emittance

ϵ_B = back surface thermal emittance

S = solar constant at D = 1

θ = angle of incidence

η = solar cell efficiency

D = solar distance (AU)

σ = Stefan-Boltzmann constant

is well suited to our needs. The equation is a simplification and assumes the temperature of outer space to be 0K. The actual temperature is near 4K, but the error generated by this assumption is less than 4ppm at T=100K and even less for higher values of T. The front surface solar absorptance of typical covered solar cells is 0.81 and the front surface total hemispherical emittance at 300K is 0.84. The emittance has a slight temperature coefficient (2×10^{-4}/K) but this will be ignored. The cells are assumed to be mounted on

a paddle type structure. For this configuration, we may assume an effective back surface total hemispherical emittance of 0.9. This is consistent with temperature differentials actually experienced on honeycomb substrates and with published emittances of black high-emittance finishes. The solar constant is taken as 0.136 $W\text{-}cm^{-2}$, a realistic value in light of recent measurements (Reference 1). The angle of incidence is assumed to be 0 (normal incidence). The power generated by the solar cells mounted on a paddle-type structure is generally dissipated elsewhere in the spacecraft. This has the effect of lowering the solar cell temperature. For Mercury and Venus, the assumed efficiencies are 0.01 and 0.06 respectively. The mean solar distances for Mercury and Venus are 0.39 and 0.72 AU respectively. The sun is treated as a point source in assuming that the inverse square law applies.

Solution of Equation 1 yields the following equilibrium temperatures (using a solar constant of 0.136 $W\text{-}cm^{-2}$): Mercury - 519K; Venus - 377K. If a solar constant of 0.1396 $W\text{-}cm^{-2}$ is preferred, the equilibrium temperatures become: Mercury - 522.4K; Venus -379K.

The calculated temperature for a conventional cell at Venus (104C) is reasonable, and worthwhile amounts of power can be expected. However, this conventional cell will be essentially inoperative at Mercury because of the high equilibrium temperature. It is necessary to reduce the input energy by some means to bring the temperature to a reasonable level.

Several methods have been proposed to limit the input energy to a solar cell for operation at Mercury (Reference 2). Tilting the solar panel is one approach, where cos ~~θ~~ in Equation 1 is reduced. This method has an advantage in that full power can be available during the entire mission, but the spacecraft attitude control to maintain proper orientation at Mercury is difficult. Another method is to limit the incident energy by reflecting a portion of it (reducing α_s in Equation 1).

This reflection can be done in either of two methods: (1) use of a bandpass filter to accept radiation where the cell is most efficient, and (2) use of a spatial filter, where a portion of the area of the cell reflects the sunlight. The bandpass filter approach is better theoretically, but practical filters fall somewhat short of ideal filters used in calculations. The spatial filter technique is easily applied and has a secondary benefit in that the reflecting portion can also be used as a contact material and thus reduce series resistance in the cell. This approach has been selected for development.

3.2 Cell Power Studies:

The optimization of the reflecting contact cell is best carried out with a digital computer. The successful application of a computer requires an equation relating cell power to cell temperature and irradiance, and an equation relating cell temperature to irradiance and thermal characteristics. The latter equation is Equation (1) in section 3.1. The former has been derived using earlier data.

As a starting point, the series of curves shown in Figure 1 was used. These curves were derived from a series of measurements on Centralab 1x2 cm cells and can be applied to 2x2 cm cells directly. The curves were drawn at constant temperature (28C) by bonding the cell to a water-cooled heat sink and monitoring temperature with a thermocouple. The source was a filtered 1000 watt tungsten landing lamp and the radiation was focussed on the cell with a large parabolic reflector. The I-V curves were made using a variable voltage source such that they could be drawn well into the reverse region. This enabled the cell under test to be its own irradiance detector, by scaling the light-generated current I_L to multiples of the I_L at AM=0, 1AU. The series resistance effect of the test leads was mathematically removed from the original curves.

To determine the effect of temperature on these curves, the voltage axis was shifted in 100 mV increments to a total shift of 400 mV. Using a temperature coefficient

of open circuit voltage of -2.26 mV/°C, these shifts correspond to temperatures of 72, 117, 161 and 205°C in addition to the original curves at 28°C. The small change in current was neglected in order to simplify the calculations.

The maximum power for each of the five temperatures and for irradiances of 1 to 8 AM=0 suns was determined from the curves using transparent overlays and slide rule calculations. The powers determined (relative) are shown in the following table:

sun / temp	1	2	3	4	5	6	7	8
28	.414	.787	1.116	1.434	1.726	1.992	2.232	2.456
72	.324	.612	.862	1.105	1.320	1.528	1.702	1.871
117	.236	.439	.617	.790	.937	1.090	1.206	1.321
161	.149	.278	.389	.493	.584	.690	.765	.834
205	.073	.138	.193	.243	.286	.343	.381	.412

The values in the table were plotted as the ordinate with the irradiance as the abcissa and the temperature as the parameter. The plots are not linear, so a "range of interest" was devised such that the expected temperature and irradiance levels would be included. Within this "range of interest", straight line approximations can be made. The graph is shown in Figure 2. Five equations were derived, one for each temperature. They are

$$28^{\circ}C \quad - P = .331S + .123$$
$$72^{\circ}C \quad - P = .245S + .123$$
$$117^{\circ}C - P = .169S + .099$$
$$161^{\circ}C - P = .101S + .086$$
$$205^{\circ}C - P = .04S \quad + .092$$

where P is the relative power and S is the irradiance in solar constants.

A graph was made, plotting the coefficient of S and the ordinate intercept against the temperature T as shown in Figure 3. A second-order polynomial was fit to the coefficients of S using the values at T=28, 117 and 205°C. This polynomial is $(2 \times 10^{-6}T^2 - 2.11 \times 10^{-3} T + .389)$. For the ordinate intercept a least squares straight line was fitted, taking the form $(-2.23 \times 10^{-4} T + .13)$. The factor 143 was added to convert the relative value at 28°C, AM=0 (0.414) to 59 mW. The complete equation is

$$P=143\left[S(2\times10^{-6}T^2-2.11\times10^{-3}T+.389)+.13-2.24\times10^{-4}T\right] \quad (2)$$

P = power in mW from a 2 x 2 cm cell

S = solar constants

T = cell temperature (°C)

The equation fits the measured data rather well. The solid triangles in Figure 2 show solutions to the equation for various values of T and S.

A program incorporating the two equations was written in the BASIC language for the General Electric MKII time sharing computer.

```
 10 LET A=.01
 15 LET E=.7
 20 LET D=.39
 25 LET C=.55
 30 LET N=.005
 40 LET B=.136/(1.8075*5.67E-12)
 50 FOR X=C TO E STEP A
 60 LET T=((B*(1-N)*(X*.1+(1-X)*.85))/D↑2)↑.25
 70 LET R=T-273.2
 80 LET S=1/D↑2
 90 LET M=143*(S*(2E-6*T↑2-2.11E-4*T+.389)+.13-2.24E-4*T)
100 IF M<0 THEN 130
110 LET P=M*(1-X)
120 PRINT X, INT(R*10-.5)/10, INT(P*100-.5)/100
130 NEXT X
140 END
```

Equation (1) is split into two parts on lines 40 and 60. The symbol X is for the fraction of the area that is

covered by a reflecting grid with a solar absorptance of 0.1. The solar absorptance of the cell active area is taken as 0.85. Equation 2 is given on line 90. Previous trials indicated that the optimum value of X lay between 0.55 and 0.7, so X was varied between these limits in 0.01 increments. It is assumed that the final power is directly proportional to the fraction of exposed area, as shown on line 110. The results of the calculations are:

Fraction Covered	Temp. (^{o}C)	Power (mW)
.55	168.2	44.26
.56	166.3	44.44
.57	164.3	44.59
.58	162.4	44.70
.59	160.4	44.78
.60	158.4	44.82
.61	156.3	44.83
.62	154.3	44.81
.63	152.2	44.75
.64	150.0	44.65
.65	147.9	44.51
.66	145.7	44.33
.67	143.5	44.11
.68	141.2	43.84
.69	138.9	43.54
.70	136.5	43.19

By inspection of the table, it can be seen that the optimum reflective area is 0.61, with a resulting equilibrium temperature of 156.3^{o} and a power of 44.83 mW. It can also be seen that for the power to be within 1% of optimum, the reflective area fraction can vary between .56 and .66.

It was mentioned earlier that a bandpass filter offered theoretical advantages for reducing the input energy to a Mercury cell. An hypothesis was formulated wherein the reflection minimum of the SiO anti-reflection coating normally applied to solar cells would be shifted to longer wavelengths where the efficiency of solar cells is higher would lower the temperature by reflecting some of the less useful short-wavelength solar radiation with a net increase in power. The currently used SiO thickness is 80 nm corresponding to a reflection minimum of approximately 600 nm. Calculations were made to

determine solar absorptance and power loss due to decreased film transmission for film thickness from 70 to 120 nm.

The variation in solar absorptance with film thickness was calculated using equations giving reflectance as a function of component indices of refraction and thickness, applied at 20 selected ordinates (Ref. 3). The reflectance equations (Ref. 4) are

$$R = \frac{r_1^2 + r_2^2 + 2r_1\, r2 \cos 2\varphi}{1 + r_1^2\, r_2^2 + 2r_1\, r2 \cos 2\varphi}$$

where $r_1 = (n_o - n_1)/(n_o + n_1)$

$r_2 = (n_1 - n_2)/(n_1 + n_2)$

R = reflectance of assembly

n_o = index of refraction of air

n_1 = index of refraction of SiO

n_2 = index of refraction of Si

$\varphi = 2\pi n_1 e/\lambda$

e = thickness of SiO

λ = wavelength

Assuming that the assembly does not transmit any radiation, the absorptance is given by A=1-R. The computer was used to solve Equation 3 for the 20 selected ordinates using index of refraction values shown in Figure 4 (Refs. 5-7) and for film thicknesses from 70 to 120 nm. As shown in Figure 5, the temperature (calculated using Equation 1) does indeed drop with increasing film thickness, and the relative power due to this temperature drop (calculated using Equation 2) does increase.

However, there is a loss in light-generated current due to the increased reflection of light in the wavelength range where the sunlight is most intense. This is demonstrated by the reflectance curves shown in Figure 6. To determine the magnitude of this loss, a short computer program was written wherein the spectral response of a bare (uncoated) cell was multiplied by both Johnsons curve and the ratio of (1-R) of the coated cell to (1-R) of bare silicon. The results were summed across the spectral range of the cell. Mathematically, this is given by

$$I = \Sigma J_{(\lambda)} * R_{(\lambda)} * \frac{1-R_1(\lambda)}{1-R_2(\lambda)} \qquad (4)$$

where I = current

$J(\lambda)$ = solar spectral irradiance (Johnson)

$R(\lambda)$ = relative response of uncoated cell

$R_1(\lambda)$ = reflectance of uncoated cell

$R_2(\lambda)$ = reflectance of coated cell

These results are also shown in Figure 5, wherein the relative power is equated to I in Equation 4. When the two relative powers are multiplied, it is apparent that no net gain is achieved by altering the A-R coating.

3.3 Series Resistance:

For operation at high levels of irradiance such as a Mercury or Venus mission, the most important loss factor is the series resistance. Consequently, for these missions, the series resistance must be minimized. Assuming that contact resistances are not improveable beyond the currently used titanium-silver system, the two elements of importance are the diffused layer-grid structure resistance and the bulk resistance. Since some 61% of the top surface of a Mercury cell must be reflective, a contact pattern can be derived using the reflecting area to minimize the series resistance.

As a starting point, Equation 5 (Reference 8)

$$S^3 + \left(\frac{2W^2}{T} * \frac{P_T}{P_S} + \frac{3T}{2}\right) S^2 + \left(4W^2 * \frac{P_T}{P_S}\right) S - \frac{4\ VT}{P_S j_{mp}} = 0 \quad (5)$$

where S = grid separation

W = cell width (1.9cm)

T = grid line thickness

P_t = sheet resistance of grid line

P_s = sheet resistance of diffused layer

V = cell voltage at operating temperature (190mV)

j_{mp} = cell current density at operating point (.26 A/cm^2)

was modified using the relationship T = 1.22S/(.78-S), which was derived from the area constraint. The resulting equation, a third order polynomial, was solved for a combination of diffused-surface sheet resistances and grid-line sheet resistances using a ROOTER program in the GE time-sharing library. The results, shown in the table below, indicate a 3 or 4 grid cell would be optimum if Equation 5

P_t	P_s	S	T	N
.005	40	.17	.38	3.3
.005	30	.20	.47	2.7
.005	25	.22	.54	2.3
.005	20	.25	.65	1.9
.002	40	.17	.39	3.2
.002	30	.20	.48	2.6
.002	25	.22	.55	2.3
.002	20	.25	.66	1.9

applies. Values of .005 and .002 ohms per square grid line resistance correspond to unsoldered and soldered titanium-silver grids. The N values are the number of grids calculated from the relationship $N=(2-S)/(S+T)$. This number must be rounded up to the next higher integer and S and T re-evaluated. Figure 7 shows a four-grid Mercury cell according to this criteria.

It is evident from inspection of Figure 7 that a more desirable grid pattern could be devised, leaving the same reflecting area and putting on more grids. Equation 5 is useful for optimizing a grid pattern where the active area is unknown, but it apparently does not apply in this case. In an attempt to arrive at a useful cell for Mercury, other configurations were investigated. The most promising solution lies in a "checkerboard" pattern, as depicted in Figure 8. The active areas are quite small, and the cell is symmetrical, with orientation during assembly unimportant.

For a Venus cell, Equation 5 was successfully applied to arrive at a cell with 10 grids. In this case, a grid-line width of .02 cm was chosen, along with a voltage of 0.3 volts and a J_{sc} of .075 A/cm^2. The calculations are shown in the table below.

Pt	P_s	S	N
.01	30	.154	10.6
.005	30	.178	9.2
.002	30	.198	8.3
.01	20	.165	9.9
.005	20	.196	8.4
.002	20	.223	7.3

The Cell Design is Shown in Figure 9.

The optical and electrical characteristics of the diffused layer are not sufficiently understood to allow a mathematical optimization. As the sheet resistance is decreased from 33 ohms per square (the empirically determined value for 1AU), the series resistance and the light-generated current both decrease. The change in series resistance is calculable and has been included in

the grid optimization studies. The loss in current is not calculable and must be determined by experiment. Starting values of 20 ohms per square for Mercury and 25 ohms per square for Venus seem reasonable.

The base resistivity is in part responsible for the series resistance of a cell, contributing about .05 ohms for a 2 x 2 cell with 10 ohm-cm base resistivity and about .01 ohms for a similar cell with 2 ohm-cm base resistivity. At a current level of 300 mA (for a Venus cell) each .01 ohm of base resistance creates a voltage drop of 3 mV equivalent to 1% in power. At a current of 400 mA (for a Mercury cell with 61% reflective), each .01 ohm of base resistance creates a voltage drop of 4 mV, equivalent to 2.1% in power. Hence, a low base resistivity is desirable. Theory indicates that lowering the base resistivity to 0.1 ohm-cm or even lower should produce good cells, with the important advantage of high open-circuit voltage. In practice, the expected voltage increase has not materialized. A few experimental cells near 0.5 ohm-cm have proven good, but these have been the exception. Based upon present state-of-art, base resistivities in the range 0.8 - 1.5 ohm-cm are suitable for both Mercury and Venus cells.

3.4 Cell Designs:

This section describes the cells designed for Mercury and Venus applications. All aspects of their design have been considered.

3.4.1 Base Resistivity and Type:

a. Mercury - 0.8 to 1.5 ohm-cm, boron doped.

b. Venus - 0.8 to 1.5 ohm-cm, boron doped.

3.4.2 Junction Characteristics:

a. Mercury - 20 ohms/sq ($\sim$ 0.6 μ), phosphorus.

b. Venus - 25 ohms/sq ($\sim$ 0.5 μ), phosphorus.

3.4.3 Contact Material:

a. Mercury - sintered titanium-silver, solderless.

b. Venus - sintered titanium-silver, solder optional.

3.4.4 Grid Pattern and Size:

a. Mercury - see Figure 8.

b. Venus - see Figure 9.

3.4.5 Antireflection Coatings:

a. Mercury - 80 nm SiO.

b. Venus - 80 nm SiO.

3.4.6 Handling Characteristics and Restraints:

a. Mercury - no restraints. Since cell is symmetrical, it can be used with any edge as the contact.

b. Venus - no restraints. Handle like conventional cells.

3.4.7 Production Cost and Implementation Time:

a. Mercury - the cost of the Mercury cell will be slightly greater than conventional cells because one additional evaporation is required. The implementation time will be the same as for other cells, being limited only by acquisition time of evaporation fixtures.

b. Venus - the cost of the Venus cell will be similar to conventional cells. The implementation time will be the same as for other cells, being limited only by acquisition time of evaporation fixtures.

3.4.8 Weight:

a. Mercury - same as conventional cell (2 x 2 cm .014 inch thick) 0.35 gram.

b. Venus - same as conventional cell (2 x 2 cm .014 inch thick) 0.35 gram; with optional solder, 0.41 gram.

3.4.8 Special Tooling:

a. Mercury - special evaporation mask required, 8 fingers, each 1.5 mm (0.060 in.) wide.

b. Venus - special evaporation mask, similar to conventional but for 10 grids.

4.0 Conclusions

Near-optimum solar cells have been designed for operation at Mercury and Venus. Several of the parameters did not lend themselves to a theoretical optimization. These parameters must be empirically treated during the experimental fabrication stage.

5.0 Recommendations

It is recommended that the analysis phase be extended to allow further analysis of the results of the experimental fabrication phase.

6.0 New Technology

No reportable items of new technology have been identified during performance of this work.

7.0 References

1. Drummond, A. J., "Precision Radiometry and its Significance in Atmospheric and Space Physics", in Advances in Geophysics, Volume 14, Academic Press (1970).

2. Ross, R. A., Jr., "Solar-Panel Approaches for a Venus-Mercury Flyby", presented at Space Technology and Heat Transfer Conference, Los Angeles, June 1970, ASME Paper 70-Av/Sp T-29.

3. Olson, O. H., "Selected Ordinates for Solar Absorptivity Calculations", Appl. Opt. 2, 109 (1963).

4. Francon, M., "Modern Applications of Physical Optics", Interscience, New York (1963).

5. Hass, G. & Salzberg, C. D., "Optical Properties of Silicon Monoxide in the Wavelength Region from 0.24 to 14.0 Microns", J. Opt. Soc. Amer. 44, 181 (1954).

6. Runyan, W. R., "Silicon Semiconductor Technology", McGraw-Hill, New York (1965), p. 198.

7. Schmidt, E., " Simple Method for the Determination of Optical Constants of Absorbing Materials", Appl. Opt. 8, 1905 (1969).

8. Crossley, P.A., et al, "Review and Evaluation of Past Solar-Cell Development Efforts", Final Report, NASA Contract NASW-1427, RCA, Princeton, N. J. (1968), Appendix 2.

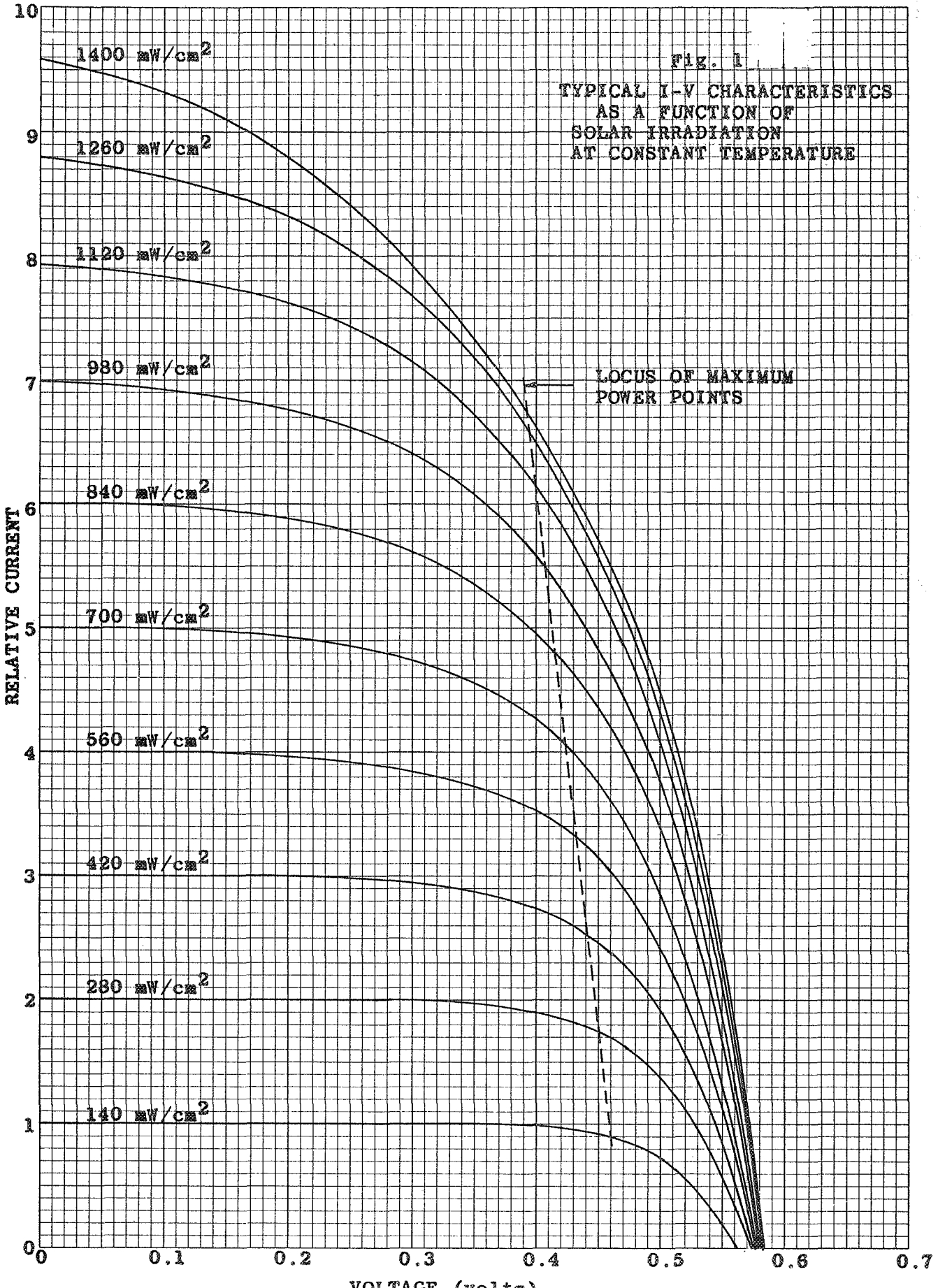
Fig. 1
TYPICAL I-V CHARACTERISTICS
AS A FUNCTION OF
SOLAR IRRADIATION
AT CONSTANT TEMPERATURE
1400 mW/cm2
1260 mW/cm2
1120 mW/cm2
980 mW/cm2
840 mW/cm2
700 mW/cm2
560 mW/cm2
420 mW/cm2
280 mW/cm2
140 mW/cm2
LOCUS OF MAXIMUM
POWER POINTS
RELATIVE CURRENT
VOLTAGE (volts)
0
1
2
3
4
5
6
7
8
9
10
0.1
0.2
0.3
0.4
0.5
0.6
0.7

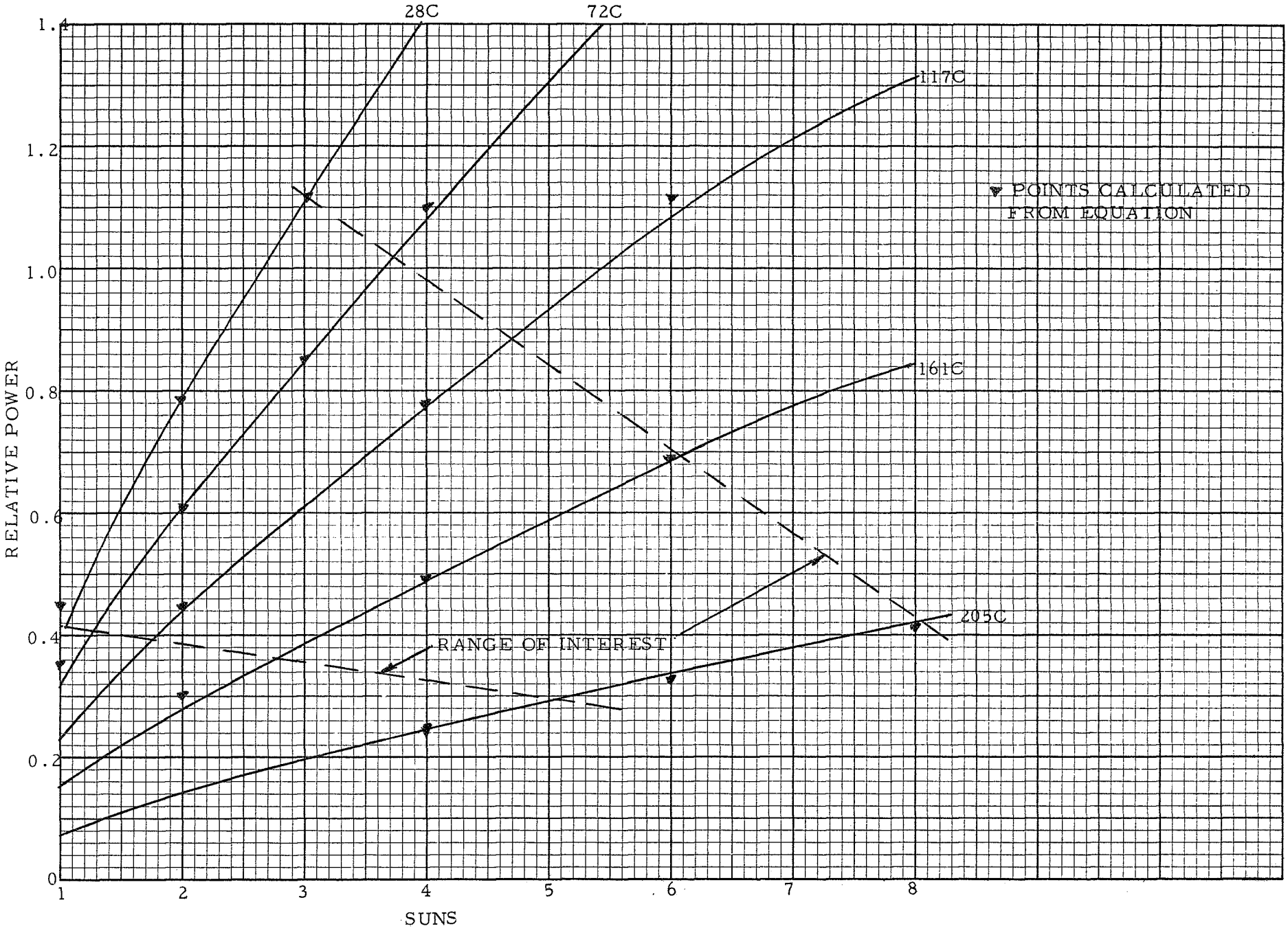

FIGURE 2. RELATIVE POWER vs. IRRADIANCE and TEMPERATURE

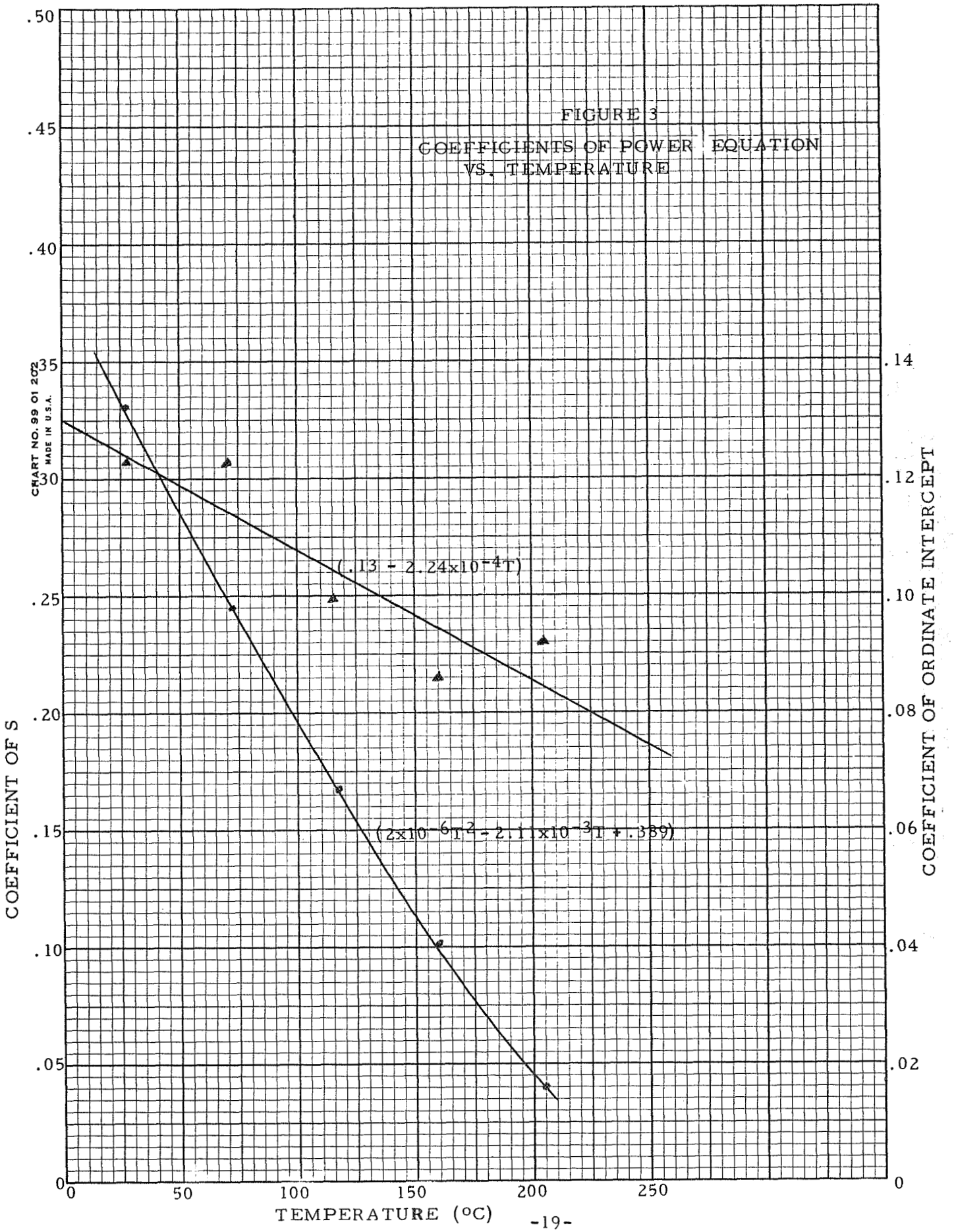
FIGURE 3
COEFFICIENTS OF POWER EQUATION
VS. TEMPERATURE
(.13 - 2.24x10⁻⁴T)
(2x10⁻⁶T² - 2.1x10⁻³T + .389)
COEFFICIENT OF S
COEFFICIENT OF ORDINATE INTERCEPT
TEMPERATURE (°C)
.50
.45
.40
.35
.30
.25
.20
.15
.10
.05
0
.14
.12
.10
.08
.06
.04
.02
0
0
50
100
150
200
250
CHART NO. 99 01 202
MADE IN U.S.A.

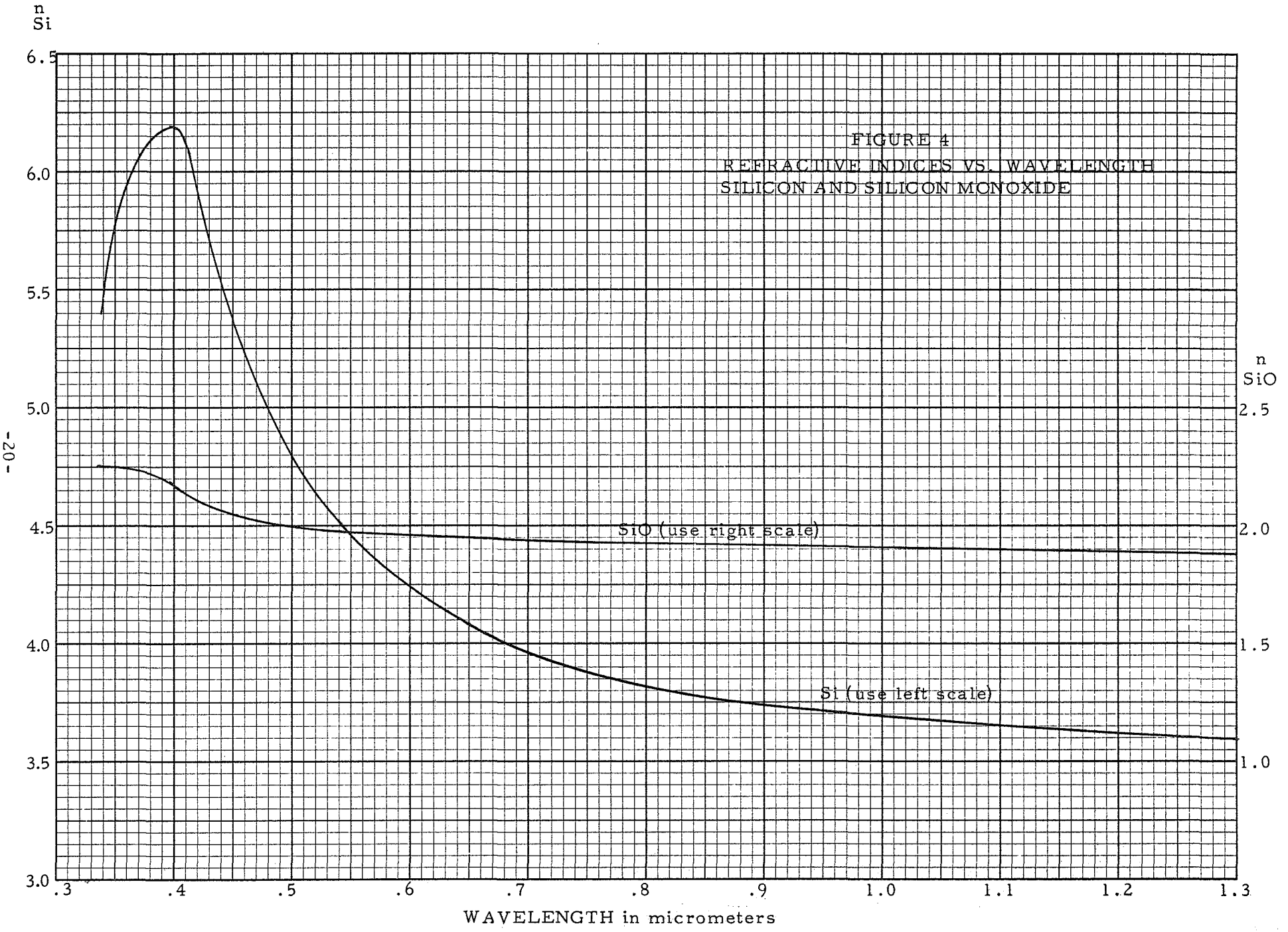

FIGURE 4
REFRACTIVE INDICES VS. WAVELENGTH
SILICON AND SILICON MONOXIDE

SiO Thickness (nm)	λ For R min (nm)	Solar Absorptance (α_s)	Equilibrium Temperature (^{o}C)	Relative Power	Power Loss Due to Coating	Overall Power
70	532	.839	151.2	.988	.992	.980
80	608	.834	150.2	1	1	1
90	684	.826	149.8	1.005	.989	.994
100	760	.822	149.4	1.009	.966	.975
110	836	.820	149.1	1.013	.937	.949
120	912	.813	148.4	1.021	.908	.927

Figure 5

FIGURE 6

ANTI-REFLECTION COATING CHARACTERISTICS

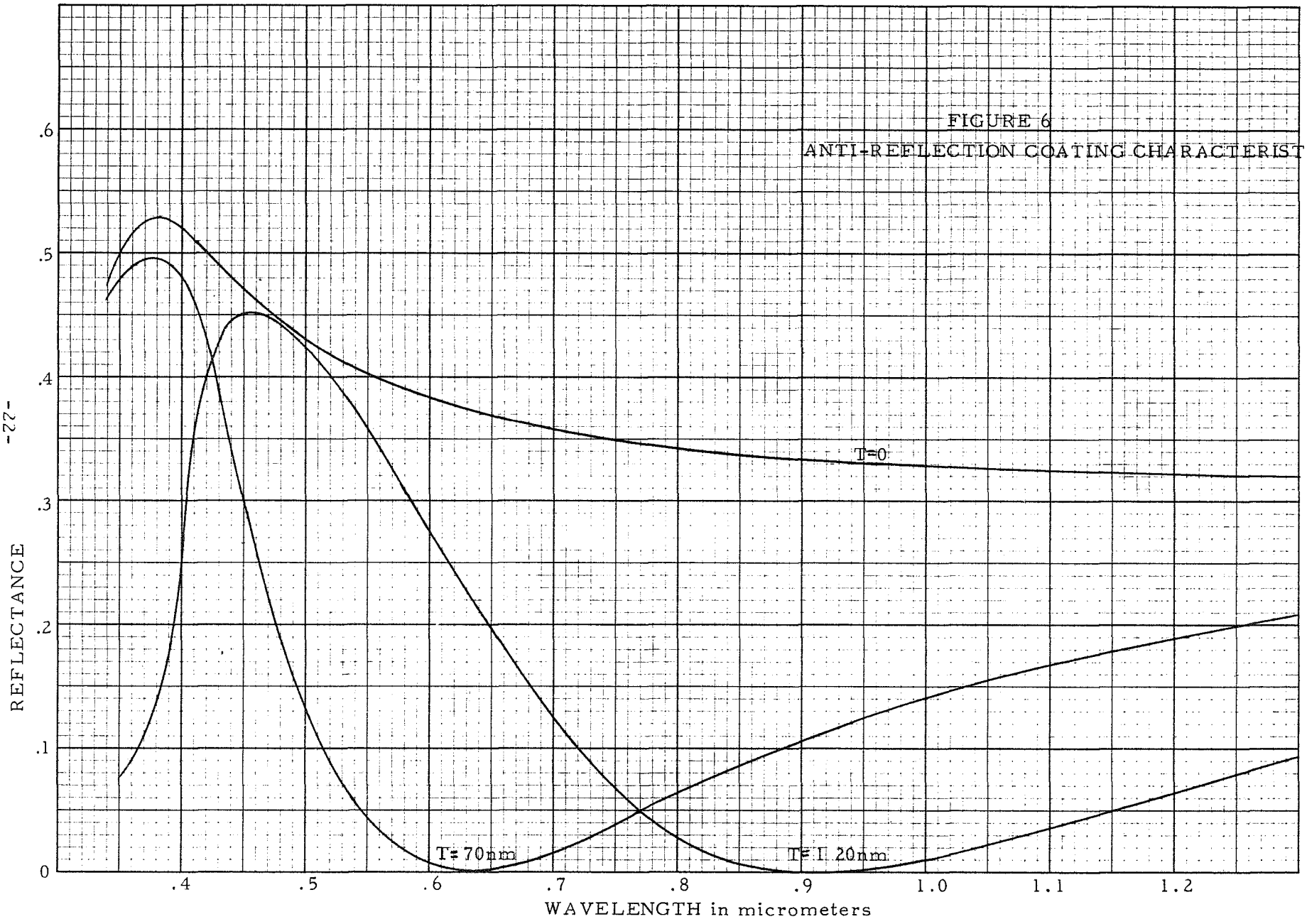

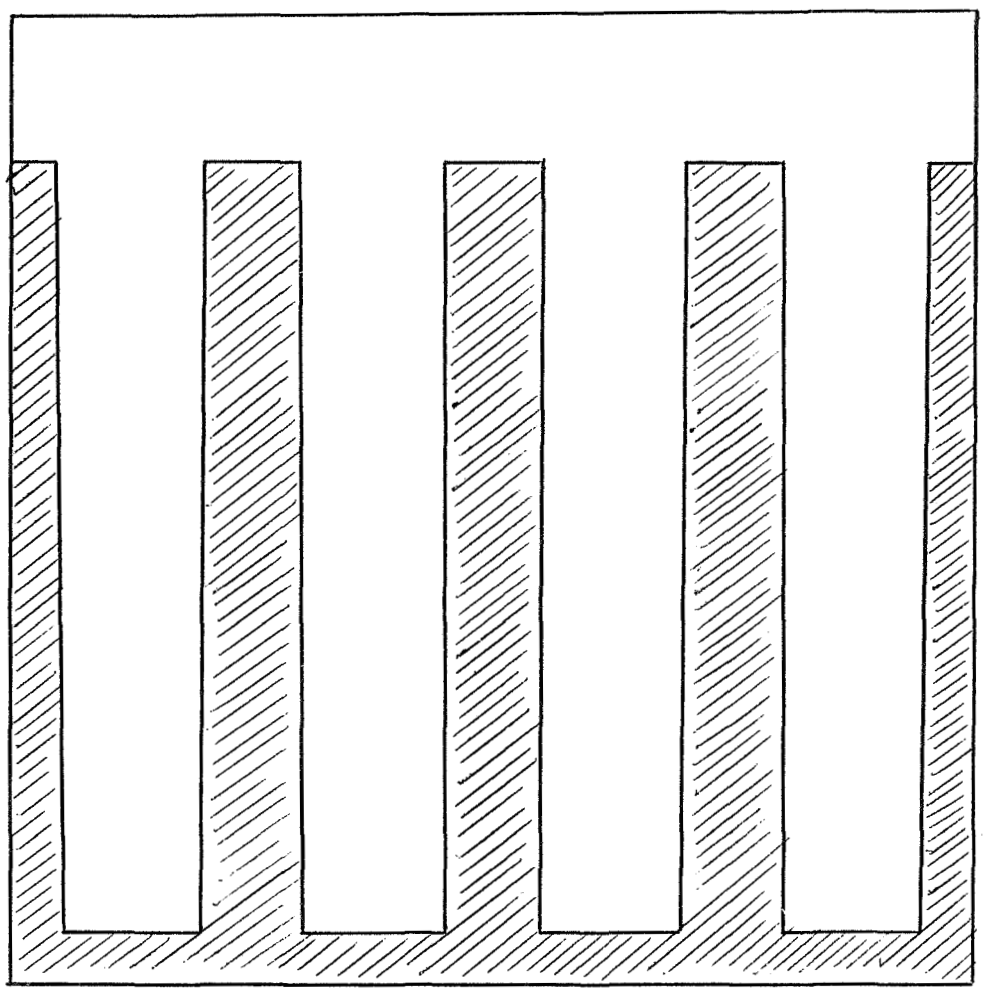

FIGURE 7

FOUR-GRID MERCURY CELL

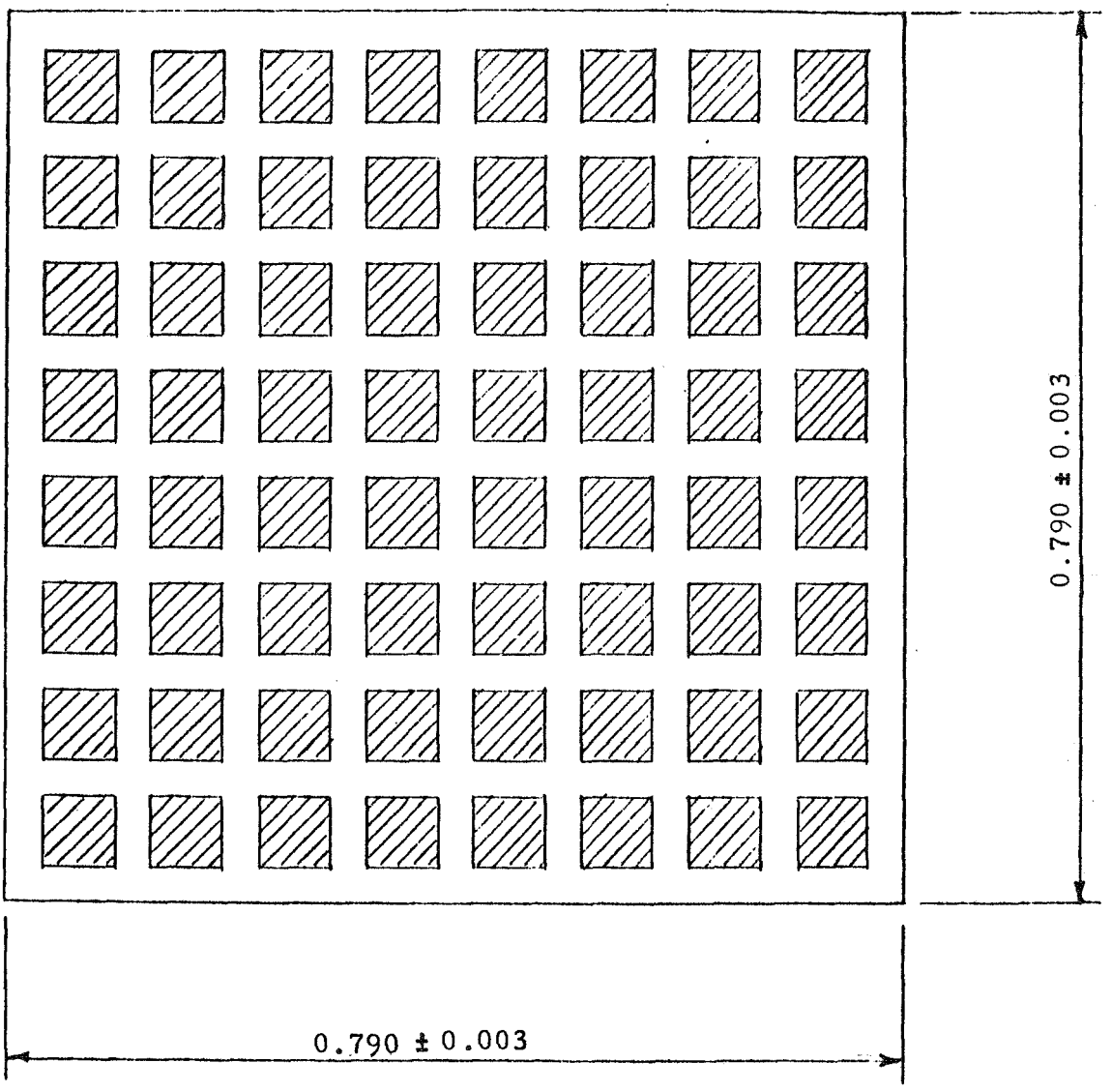

EACH ACTIVE AREA 0.060 x 0.060
SPACING 0.035

FIGURE 8

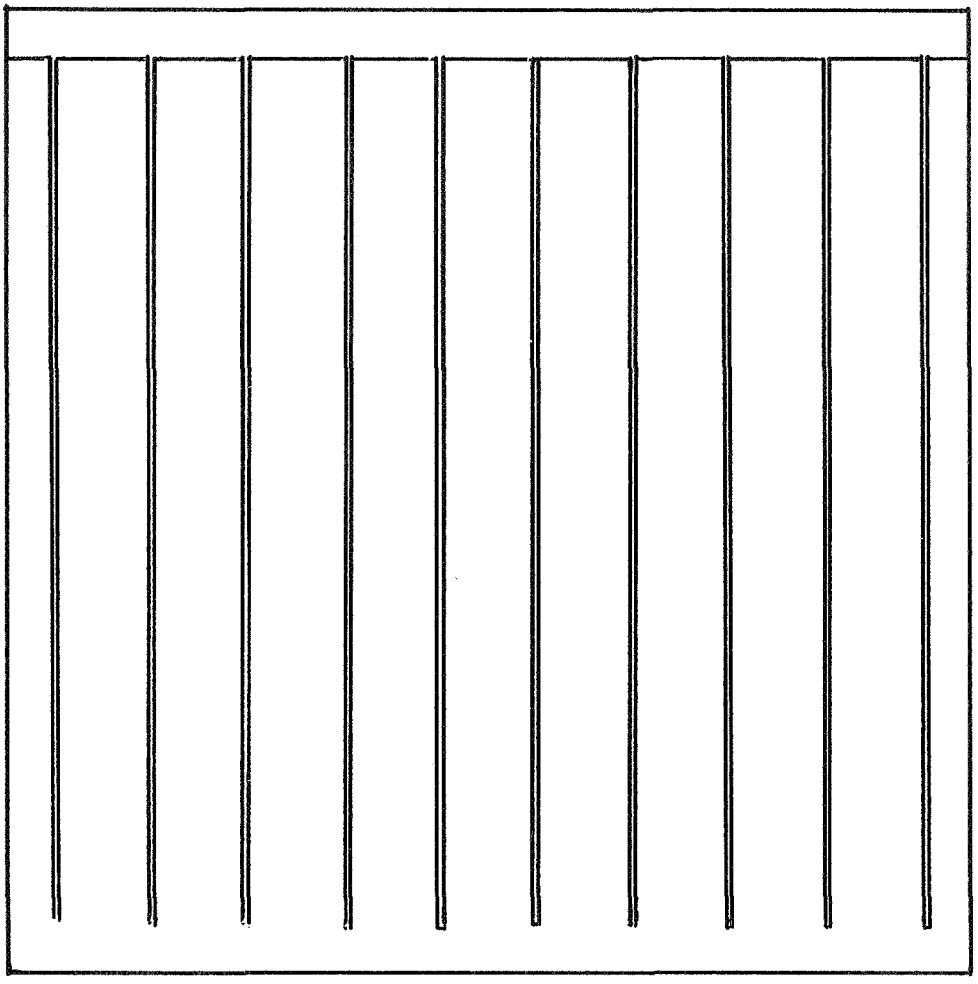

FIGURE 9. GRID PATTERN FOR VENUS CELL